

The influence of oxygen concentration on the rheological properties and flow of whole human blood

A. Zupančič Valant¹ · L. Ziberna² · Y. Papaharilaou³ · A. Anayiotos⁴ · G.C. Georgiou⁵

Received: 30 March 2016 / Revised: 1 September 2016 / Accepted: 13 September 2016 / Published online: 26 September 2016
© Springer-Verlag Berlin Heidelberg 2016

Abstract Variations in blood oxygen concentrations are not only part of the normal physiology but they may also indicate various pathological conditions. In the present work, we examined the influence of oxygen concentration on the rheological properties of whole human blood. Blood samples were taken from two healthy donors, a male and a female, with hematocrits 0.47 and 0.42, respectively. In addition to the original samples of normal oxygen concentration (normoxemia), samples of different blood oxygen level were also prepared by using the perfusion cell equipped with a gas supply to induce either hypoxemia by driving out the oxygen

saturation of blood by nitrogen or hyperoxemia by saturating blood with oxygen. The rheology of the samples was measured using a Physica MCR 301 rheometer equipped with a sensor designed for hemorheology. The rheological results showed that oxygen-depleted blood exhibited lower viscosity and a lower yield stress when fitted to the Herschel-Bulkley constitutive model. Blood flow simulations of the effect of oxygen concentration on the local hemodynamics were also carried out in an idealized axisymmetric 75 % stenosis and in a realistic carotid bifurcation geometry constructed from MRI images obtained from a healthy male volunteer. The modified Herschel-Bulkley model with the Papanastasiou regularization was used to account for both the shear thinning and finite yield stress properties of blood. The results of this work showed that oxygen concentration affects the rheology and flow behavior of blood, suggesting compensatory responses under hypoxic conditions leading to a lower blood viscosity.

✉ G.C. Georgiou
georgios@ucy.ac.cy

L. Ziberna
lovro.ziberna@mf.uni-lj.si

Y. Papaharilaou
yannisp@iacm.forth.gr

A. Anayiotos
andreas.anayiotos@cut.ac.cy

Keywords Hemorheology · Blood · Oxygen concentration · Herschel-Bulkley model · Hemodynamics · Carotid bifurcation

¹ Department of Chemical, Biochemical and Environmental Engineering, Faculty of Chemistry, University of Ljubljana, Askerceva 5, SI-1000 Ljubljana, Slovenia

² Institute of Pharmacology and Experimental Toxicology, Faculty of Medicine, University of Ljubljana, Korytkova 2, SI-1000 Ljubljana, Slovenia

³ Institute of Applied and Computational Mathematics, Foundation for Research and Technology Hellas (FORTH), PO Box 1527, 71110 Heraklion, Crete, Greece

⁴ Department of Mechanical Engineering and Materials Science and Engineering, Cyprus University of Technology, Limassol 3503, Cyprus

⁵ Department of Mathematics and Statistics, University of Cyprus, PO Box 20537, 1678 Nicosia, Cyprus

Introduction

Blood is a biological fluid that delivers nutrients and oxygen to living cells and removes their metabolic wastes (Lykov et al., 2015). Understanding its rheological and flow properties (that is hemorheology) is necessary in developing improved diagnostic and therapeutic tools for cardiovascular, hematological, and other diseases or disorders and in advancing biomedical and clinical applications, such as drug delivery (Fedosov et al., 2011).

Blood is a concentrated suspension of several formed cellular elements, red blood cells (RBCs), white blood cells, and

platelets in plasma. Blood plasma is an aqueous polymeric and ionic solution of constant viscosity, i.e., it is a Newtonian fluid, in shear flow. Recently, it has been established that plasma shows significant viscoelastic effects in elongational flow in a capillary breakup extensional rheometer and also in a microfluidic contraction-expansion device (Brust et al., 2013). Fibrinogen, one of the various proteins in plasma, is known to affect the rheological properties of blood by promoting the aggregation of RBCs at low shear rates (Picart et al., 1998; Apostolides and Beris, 2014). Unlike plasma, blood is a complex non-Newtonian fluid. Its viscosity and other rheological properties depend on many factors; the most important of which are the hematocrit, the flow which affects the behavior of RBCs and the temperature (Caballero and Lain, 2015). The hematocrit, defined as the volume percentage of RBCs in whole blood, has a more pronounced effect on viscosity at high shear rates (Kim et al., 2009; Smith et al., 2015). Blood viscosity increases with hematocrit and decreases quickly with temperature (Rand et al., 1964; Valant et al., 2011). Flow affects the deformation and the aggregation-disaggregation of RBCs (Brun et al., 2013; Bertoluzzo et al., 1999) which have a dramatic effect on the blood viscosity. Apostolidis and Beris (2016) reported that cholesterol and triglycerides contribute to cardiovascular diseases by increasing blood viscosity. The viscosity of whole human blood also varies with hydration/dehydration in exercising (Diaw et al., 2014).

Acute changes in the oxygen concentration of whole blood also lead to changes in the rheology and flow behavior of blood. Smith et al. (2015) reported that aerobic training (not resistance training) is associated with a hemorheological profile that promotes both oxygen transport and delivery independent of hematocrit. Variations in blood oxygen concentrations can be part of the normal physiology, e.g., difference in oxygen levels in arterial versus venous blood, during strenuous physical exercise, as well as in other conditions (De Cort et al., 1991). Hypoxia, i.e., reduced oxygen concentration in tissues, is often considered as the common cause of tissue and cell injury (Guner et al., 2013). It may be observed in physiological and pathophysiological conditions such as severe exercise, air travels, repeated exposure to high altitude followed by returning to sea level, and obstructive sleep apnea (Guner et al., 2013). In vivo experiments showed that both blood viscosity and erythrocytes aggregation index in mice increase when they are exposed to acute hypoxic hypoxia for a brief period (5–11 min) (Zhang et al., 2012).

The experiments of Yelmen et al. (2011) on male rats placed in a hypobaric chamber (5 h/day, 5 days/week, 5 weeks) suggested that chronic long-term intermittent hypobaric hypoxia (CLTIHH) elevated whole blood viscosity by increasing plasma viscosity, fibrinogen concentration, and hematocrit value and thus CLTIHH may be responsible for hemorheologic changes in human subjects exposed to intermittent high altitude or with severe obstructive sleep apnea.

This observation can be explained by a physiological mechanism. Chronic hypoxia leads to increased erythropoietin secretion, which increases the erythrocyte production and thus increases the hematocrit level (Benderro and LaManna, 2013). Increase of blood viscosity after intermittent exposure of rats to hypobaric hypoxia (simulated altitude) was also reported by Núñez-Espinosa et al. (2014) who noted that other rheological parameters, such as higher blood elasticity and shorter relaxation time, may contribute to compensate for this augmentation. Similarly, Kang et al. (2016) reported that intermittent and continuous hypoxia increase whole blood viscosity and promote the platelet aggregation in rats and that, in chronic cases, the former has a greater effect on blood rheology. In contrast, the experiments of Esteva et al. (2009) showed that intermittent hypobaric hypoxia in rats (4 h/day, 5 days/week until 22 days of hypoxia exposure in a hypobaric chamber at a simulated altitude of 5000 m) does not affect apparent blood viscosity. Although the level of hemoglobin and hematocrit increased, blood viscosity remained unaltered due to the long-term compensatory responses on the erythrocyte level. Esteva et al. (2009) concluded that intermittent hypobaric hypoxia has a deep but transitory effect on red cell parameters and a very moderate effect on blood rheological behavior. All in all, interactions between blood oxygen level and rheological properties are not fully understood. In fact, there is still a knowledge gap in understanding the direct correlation between acute hypoxia and rheological properties of blood (Caillaud et al., 2002) and, therefore, further research is needed. Studying the hemorheology and hemodynamics at different oxygen concentrations may also shed light on the pathophysiological regulation of blood properties on the level of erythrocytes.

As already mentioned, blood exhibits non-Newtonian characteristics, i.e., shear thinning (Merrill et al., 1969), viscoelasticity (Vlastos et al., 1997), thixotropy (Dintenfass, 1962), and yield stress (Cokelet et al., 1963). The non-Newtonian properties of blood are reviewed in detail in the recent papers by Dimakopoulos et al. (2015), Bessonov et al. (2016) and Sousa et al. (2016). At low shear rates, RBCs tend to aggregate forming column-like structures called rouleaux. Shear thinning is caused by the disaggregation of the rouleaux and the alignment of individual RBCs at moderate and higher shear rates (Chien et al., 1967). Blood viscoelasticity is attributed to the reversible deformation of the RBCs three-dimensional microstructures and to the ability of the RBCs elastic membranes to store and release elastic energy (Thurston, 1996; Caballero and Lain, 2015). Thixotropy, i.e., the variation of viscosity with time at constant low shear, is mainly due to the fact that rouleaux aggregation and disaggregation are not instantaneous and thus the material properties are time dependent (Caballero and Lain, 2015).

As a suspension, blood also exhibits yield stress under physiological conditions, i.e., it flows only if the stress

exceeds a threshold value. The macroscopic yield stress is attributed to the formation of rouleaux aggregates and 3D complex networks at low shear rates (Apostolidis and Beris, 2014; Fedosov et al., 2011; Bessonov et al., 2016). In addition to experimental evidence (Cokelet et al., 1963; Merrill et al., 1969; Copley et al., 1973), the existence of a yield stress is also supported by coarse-grained molecular dynamics simulations (Fedosov et al., 2011). According to Picart et al. (1999), the best predictor of yield stress in systemic sclerosis is the ratio of albumin to globulins. Blood yield stress is known to increase with certain diseases, such as systemic sclerosis, polycythemia, and diabetes, and this may be used for diagnostic purposes (see Sousa et al. (2016) and references therein). Apostolidis and Beris (2014) showed that the threshold hematocrit value for the appearance of yield stress is a function of the fibrinogen concentration and developed accurate parametric representations relating blood yield stress and viscosity to hematocrit, fibrinogen concentration, and temperature.

For the purposes of the present study, we have chosen to use a generalized Newtonian constitutive equation instead of a time-dependent (i.e., viscoelastic/thixotropic) model which is more appropriate given the pulsatile flow conditions in the human vascular network. As noted by Apostolidis and Beris (2014), the most sophisticated viscoelastic constitutive equations for blood fail to account explicitly for yield stress and viscoplasticity. The most popular constitutive equations endowed with yield stress and describing shear thinning are the Casson and Herschel-Bulkley models (Mitsoulis, 2007). The latter model is the combination of the Bingham plastic and the power-law constitutive models. It involves three material parameters, the yield stress, τ_0 , the consistency index, k , and the power-law exponent, n , and relates the viscous stress tensor, $\boldsymbol{\tau}$, to the rate of strain tensor, $\dot{\boldsymbol{\gamma}} \equiv \nabla \mathbf{u} + (\nabla \mathbf{u})^T$ where \mathbf{u} is the velocity vector, as follows:

$$\left. \begin{aligned} \dot{\boldsymbol{\gamma}} &= \mathbf{0}, & \tau &\leq \tau_0 \\ \boldsymbol{\tau} &= \left(\frac{\tau_0}{\dot{\gamma}} + k \dot{\gamma}^{n-1} \right) \dot{\boldsymbol{\gamma}}, & \tau &> \tau_0 \end{aligned} \right\} \quad (1)$$

where the magnitudes of $\boldsymbol{\tau}$ and $\dot{\boldsymbol{\gamma}}$, denoted by τ and $\dot{\gamma}$, respectively, are defined by

$$\tau \equiv \sqrt{\boldsymbol{\tau} : \boldsymbol{\tau} / 2} \quad \text{and} \quad \dot{\gamma} \equiv \sqrt{\dot{\boldsymbol{\gamma}} : \dot{\boldsymbol{\gamma}} / 2} \quad (2)$$

It is clear that while in the unyielded zone, the viscosity is infinite and in the yielded zone, it is given by

$$\eta(\dot{\gamma}) = \frac{\tau_0}{\dot{\gamma}} + k \dot{\gamma}^{n-1} \quad (3)$$

The Bingham plastic constitutive equation is recovered from Eq. (1) when $n = 1$. If additionally the yield stress is zero, the

Newtonian model is recovered. For $n < 1$, the viscosity is a monotonic decreasing function of the shear rate (shear thinning). It is clear that in the limit $\dot{\gamma} \rightarrow 0$, the viscosity becomes unbounded. The existence of a true yield stress may have been the subject of a long debate (Barnes, 1999), but this is also widely accepted as useful notion for practical applications. In the case of hemorheology, Apostolidis and Beris (2014) also pointed out that, in addition to the overwhelming experimental evidence, the yield stress may be more easily connected to physiological parameters. In a subsequent work, Apostolidis et al. (2015) proposed a thixotropic model accounting for the additional yield-strengthening effect attributable to the RBC rouleaux structures developed within blood.

The objectives of the present work were (a) to investigate the effect of acute changes in blood oxygenation on the hemorheological properties and (b) to investigate the effect of blood oxygenation level on blood flow. To achieve the first objective, measurements of rheological properties were conducted on whole blood samples obtained from two healthy volunteers and prepared in the laboratory to obtain oxygenation levels different from the normoxic one, i.e., acute hypoxic (oxygen-depleted blood) and hyperoxic (oxygen-saturated blood). The rheological measurements are presented in “[Rheological measurements](#)” where the experimental data are fitted to the Herschel-Bulkley constitutive equation. The experiments showed that viscosity and yield stress increase with oxygen concentration. It should be noted that a thixotropic/viscoelastic model is more appropriate in modeling transient blood flow in the carotid bifurcation, but its use would require a series of experimental measurements for the determination of the additional parameters at different oxygen levels. Such an endeavor is out of the scope of the present work and we thus resort to the Herschel-Bulkley constitutive equation. To address the second objective, the calculated material parameters are then used in numerical simulations of the flow of blood with different oxygen concentrations in an idealized axisymmetric stenosis and in a realistic carotid bifurcation. The numerical method and the results are presented and discussed in “[Numerical simulations and discussion](#).” The impact of oxygen concentration in the case of the carotid bifurcation was found to be weak. In the case of the stenosis, the recirculation zone was found to reduce in size. The conclusions of this work are discussed in “[Concluding remarks](#).”

Rheological measurements

Rheological measurements have been carried out on blood samples taken from two healthy donors, a male with hematocrit 0.47 (Volunteer A) and a female with hematocrit 0.42 (Volunteer B), as measured by the automated hematology analyzer (Beckman Coulter LH 750). Blood samples were obtained by venipuncture and were anticoagulated with EDTA.

Samples with different oxygen concentrations were prepared in the laboratory by using the perfusion cell equipped with gas supply to (i) drive out the oxygen by nitrogen (hypoxia) (ii) or to fully saturate blood with oxygen (hyperoxia). To induce hypoxic conditions, we have used the nitrogen degasification approach, i.e., the removal of any dissolved gasses from blood by bubbling it with an inert gas. To obtain complete substitution, we bubbled freshly collected blood with nitrogen for 20 min at a rate of 3 bubbles/s. Indeed, nitrogen purging for 20–40 min at flow rate of 25 mL/s was found to be the most effective oxygen removal method from water solutions (Butler, 1994) in comparison to other oxygen removal approaches, such as boiling at 1 atm, boiling under reduced pressure, or sonification under reduced pressure, which could damage red blood cells and thus made hemorheological experiments impossible. Therefore, bubbling with nitrogen is the optimal approach for our experimental design—keeping blood intact and absent of oxygen. Similarly, another study used helium for 30 min to obtain complete oxygen removal, which resulted in the complete deoxygenation of red blood cell hemoglobin ($pO_2 < 0.0021$ mmHg) (Zolla, 2013). Moreover, the degasification approach also showed the absence of any erythrocyte damage (Longo et al. 2014). However, we did not use the oximeter to control the level of oxygen—therefore, we use the word hypoxia and not anoxia (complete absence of oxygen). The same applies to hyperoxia experimental conditions, where we bubbled the blood for 20 min with oxygen. Again, we did not use oximeter to quantify the partial oxygen pressure in the blood. According to the literature, both approaches should suffice to obtain complete oxygen removal or saturation of the blood, correspondingly.

The experiment was carried out in *in vitro* settings, which enabled better control of the oxygen concentration; it was not open to the atmosphere to avoid infiltration of oxygen or nitrogen. Whole blood samples of each donor were taken 2 h before the rheological measurements. Samples were mixed gently and put on a roller mixer until the experiment. The rheological properties were measured at 37 °C using a Physica MCR 301 stress-controlled rotational rheometer (Anton Paar, Graz, Austria), equipped with a sensor designed for hemorheology, i.e., a coaxial double-gap cylinder system (DG 26.7/Ti), which has been perfused with nitrogen for hypoxia and oxygen for hyperoxia.

For all blood samples, the rheological tests were repeated at least three times with fresh blood to ensure that the deviations in flow curves due to different oxygen concentration are repeatable. The rheological data for volunteers A (male) and B (female) at different oxygen levels, i.e., whole blood, blood saturated with oxygen, and blood saturated with nitrogen, are shown in Figs. 1 and 2, respectively. It can be observed that very high repeatability was obtained for normal human blood, slightly lower for fully saturated blood with oxygen and lower for blood perfused with nitrogen (without oxygen). The

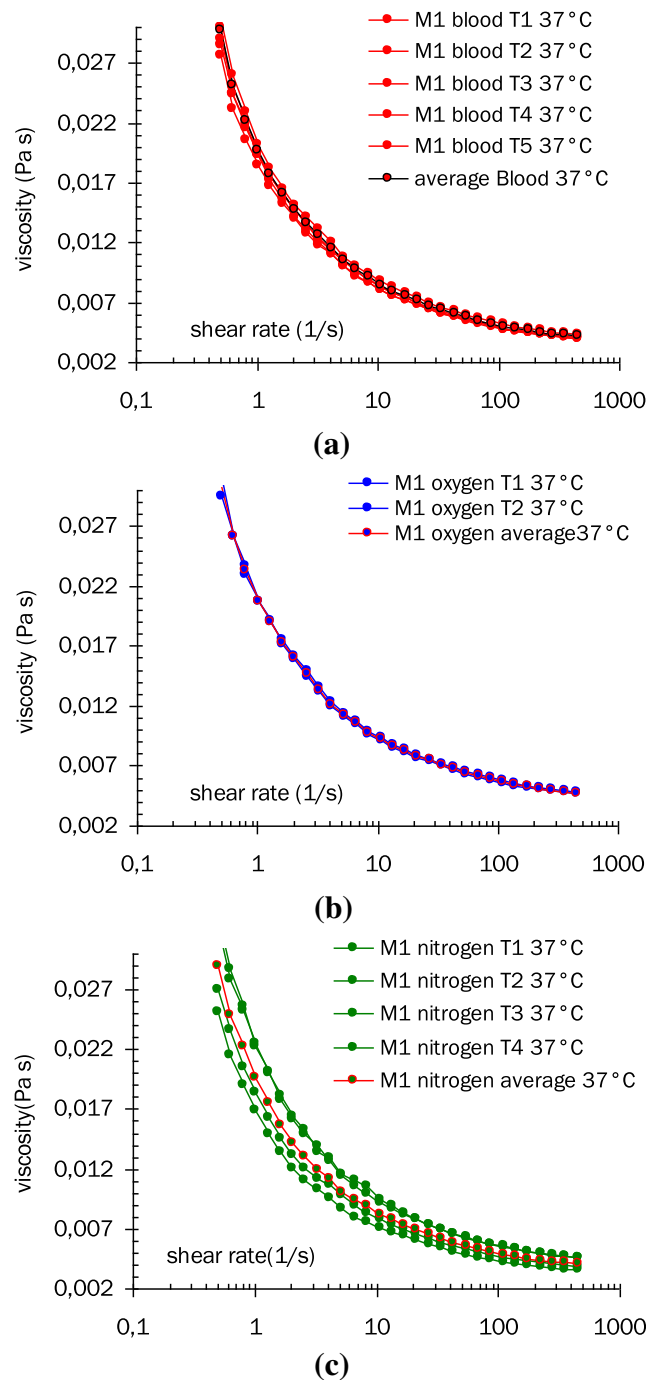


Fig. 1 Measured viscosities in different rheological tests and averaged curves for the male volunteer (A): **a** whole human blood; **b** blood saturated with oxygen; **c** blood saturated with nitrogen

poorer repeatability of the experimental measurements on the depleted samples indicates that further research is required in order to optimize the protocol for the preparation of the blood samples. The viscosities of the blood samples were determined from average values of experimental data (three repetitions) at each shear rate. Flow curves of the two blood samples at different oxygen levels are shown in Fig. 3. From the rheological data, it is clearly seen that blood without

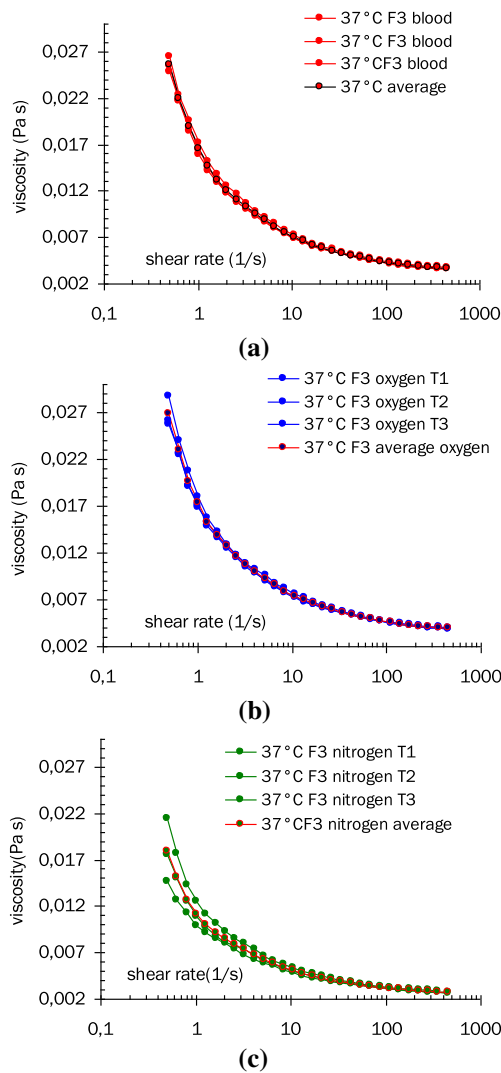


Fig. 2 Measured viscosities in different rheological tests and averaged curves for the female volunteer (B): **a** whole human blood; **b** blood saturated with oxygen; **c** blood saturated with nitrogen

oxygen exhibited lower viscosity and modified flow curve, whereas the flow curves of blood saturated with oxygen were slightly higher. The deformability of red blood cells can largely reduce the blood viscosity, thus it can be speculated that the changes in hemoglobin saturation (due to different oxygen level) can lead to conformational changes. These can affect mechanical properties of RBC, and thereby also their deformability. In human blood, hemoglobin represents an essential structural component of the red blood cell. Hemoglobin has an oxygen binding capacity and can bind up to four oxygen molecules. It has a quaternary structure, which consists of four globular protein subunits, with a specific folding pattern enabling heme binding, which binds oxygen. Upon oxygen binding, there is a slight conformational shift; indeed, hemoglobin molecule can be saturated with the oxygen (oxyhemoglobin) or desaturated (deoxyhemoglobin). Interestingly, hemoglobin can exist in two forms, influenced

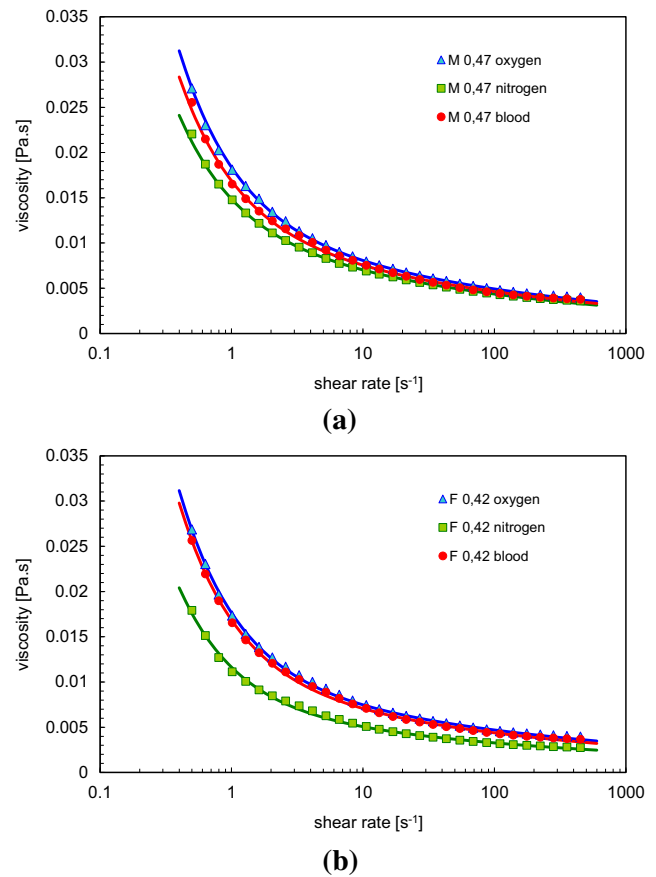


Fig. 3 Blood viscosity at different oxygen levels, i.e., oxygen-fully saturated, nitrogen-without oxygen and whole human blood: **a** male volunteer (A); **b** female volunteer (B). The solid lines correspond to the optimal fitting with the Herschel-Bulkley model

by local stimuli such as CO₂ concentration, pH, and others, which can switch conformation of the molecule. In one conformation (R form), hemoglobin can better bind oxygen; while in the other (T-form), oxygen is being released (King 2015). In this manner, hypoxia or hyperoxia can lead to conformational changes of hemoglobin molecules inside the RBCs, and so it can be speculated that these hemoglobin conformational changes also influence the erythrocyte deformability and deformation and thereby affect the whole blood rheological properties.

In all samples of Fig. 3, the viscosity decreases with shear rate, i.e., all samples are shear thinning. As the shear rate tends to zero, the viscosity appears to increase rapidly, an asymptotic behavior indicative of the presence of yield stress (Yeow et al., 2002). Hence, the rheological data for the two samples have been fitted to the Herschel-Bulkley model using non-linear regression (Excel Solver). The calculated values of the three material parameters corresponding to the different oxygenation cases of the two blood samples are tabulated in Table 1. The corresponding fittings are shown in Fig. 3 together with the averaged experimental data. The values of the power-law exponent ranged from 0.810 to 0.828 for the male

Table 1 Parameters of the Herschel-Bulkley model corresponding to the different cases of rheological measurements taken at 37 °C

Volunteer A (Htc = 0.47, T = 37 °C)			
	Case A1 (blood)	Case A2 (oxygen)	Case A3 (nitrogen)
τ_0 (Pa)	0.00610	0.00725	0.00530
k (Pa s ⁿ)	0.01086	0.01111	0.00960
n	0.810	0.820	0.828
Volunteer B (Htc = 0.42, T = 37 °C)			
	Case B1 (blood)	Case B2 (oxygen)	Case B3 (nitrogen)
τ_0 (Pa)	0.00760	0.00799	0.00522
k (Pa s ⁿ)	0.00925	0.00965	0.00641
n	0.834	0.839	0.850

sample and from 0.834 to 0.850 for the female sample. These variations are too small to indicate any trend. In any case, the power-law exponent decreases with increasing hematocrit and it has the lower values for normal human blood. As for the yield stress, both the lowest and highest values, 0.00522 and 0.00799 Pa, were obtained with the female sample in the nitrogen- and oxygen-saturated cases, respectively. It should be noted that the reported values for the whole blood yield stress vary greatly from 0.002 to 0.4 Pa (Dintenfass, 1971). For all oxygen-depleted blood samples, the values of the consistency index and the yield stress were lower and for the oxygen-saturated samples, the values of these two material parameters slightly higher than those of the untreated human blood. It can also be observed that the influence of oxygen concentration on the viscosity curves, as well as on the material parameters, mainly the consistency index, was more pronounced at lower hematocrit, i.e., for the female sample. From the experimental data, it can be deduced that oxygen concentration affects the deformability of red blood cells.

Numerical simulations and discussion

As already mentioned, we carried out numerical simulations of the flow of blood of different oxygen concentrations in an idealized axisymmetric stenosis and in a realistic carotid bifurcation. The arterial walls were assumed rigid and blood was modeled as an incompressible fluid with a density $\rho = 1050 \text{ kg/m}^3$ at all oxygen concentrations.

For the numerical solution of the continuity and momentum equations governing the three-dimensional, time-dependent incompressible flow, we used the finite volume code Fluent v12.0 (Ansys Inc.). Blood is treated as a rheologically homogeneous material which is a valid assumption in vessels with diameter larger than approximately 200 μm in which case the equations of motion can be used under the continuum hypothesis (Popel and Johnson, 2005). In vessels

of a smaller diameter, a two-phase model is necessary. In order to overcome the inherent singularity exhibited by the discontinuous Herschel-Bulkley model and the associated implementation difficulties in computational codes, we adopted the regularized version of the constitutive Eq. (3), as proposed by Papanastasiou (1987):

$$\boldsymbol{\tau} = \left\{ \frac{\tau_0 \left(1 - e^{-m\dot{\gamma}} \right)}{\dot{\gamma}} + k\dot{\gamma}^{n-1} \right\} \dot{\boldsymbol{\gamma}} \quad (4)$$

where m is the stress growth parameter. Equation (5) is valid uniformly at all levels of $\dot{\gamma}$ and provides a satisfactory approximation of the Herschel-Bulkley model for sufficiently large values of m . It should be noted, however, that the value of m must be chosen carefully, since very large values might lead to convergence difficulties. Here, a value of $m = 1000 \text{ s}^{-1}$ was used. Given that the determination of the so-called unyielded ($\tau \leq \tau_0$) and yielded regions ($\tau > \tau_0$) in the flow domain are not of interest in the present work, this value of m is sufficiently high. A discussion of the advantages and the disadvantages of regularization methods and the alternative approaches is provided in the recent review by Balmforth et al. (2014).

For comparison purposes, we have calculated the characteristic viscosity corresponding to the characteristic shear rate (not the nominal high shear rate value) defined by $\dot{\gamma}_c = 8\bar{u}/(3R)$, where \bar{u} is the averaged mean inlet velocity and R is the tube radius. Using $R = 3 \text{ mm}$ and $\bar{u} = 0.1 \text{ ms}^{-1}$ for the stenosis and $R = 2.973 \text{ mm}$ and $\bar{u} = 0.169 \text{ ms}^{-1}$ for the carotid bifurcation, the values of the characteristic shear rate were found to be 88.9 and 151.58 s^{-1} , respectively. The characteristic viscosity was then calculated as follows:

$$\eta_c = \eta(\dot{\gamma}_c) = \frac{\tau_0}{\dot{\gamma}_c} \left(1 - e^{-m\dot{\gamma}_c} \right) + k\dot{\gamma}_c^{n-1} \quad (5)$$

The dimensionless numbers of the flow, i.e., the Reynolds number, Re , and the Bingham number, Bi , were spatiotemporally averaged as follows:

$$Re \equiv \frac{2\rho\bar{u}R}{\eta_c} \quad \text{and} \quad Bi \equiv \frac{2\tau_0R}{\eta_c\bar{u}} \quad (6)$$

The calculated values of Re , Bi , and η_c for volunteer B are tabulated in Tables 2 and 3 for the stenosis and carotid bifurcation, respectively. With the above scalings, the dimensionless growth parameter of the Papanastasiou regularization, defined by $M \equiv m\bar{u}/R$, is equal to 33,333 and 56,845 for the flows in the stenosis and in the carotid bifurcation, respectively. The latter values are rather high and ensure a good approximation of the ideal Herschel-Bulkley model (Mitsoulis, 2007).

Table 2 Dimensionless numbers for flow in the idealized stenosis for Volunteer B (Htc = 0.42)

Number	Case B1 (blood)	Case B2 (oxygen)	Case B3 (nitrogen)
Re	140.72	131.93	189.16
Bi	0.1019	0.1004	0.0941
η_c	0.0045	0.0048	0.0033

Table 3 Dimensionless numbers for flow in the carotid bifurcation for Volunteer B (Htc = 0.42)

Number	Case B1 (blood)	Case B2 (oxygen)	Case B3 (nitrogen)
Re	259.28	242.42	345.42
Bi	0.0657	0.0646	0.0601
η_c	0.0041	0.0044	0.0031

As in our previous work (Valant et al., 2011), from the discrete Fourier series of the physiological volumetric flow rate measured in vivo by MRI (Fig. 4), the fully developed, time-varying velocity profile was computed using Womersley’s derivation and was then imposed as the time-dependent inflow boundary condition. For the in vivo MR measured flow waveform shown in Fig. 4, the period is $T=1.032$ s. The Womersley parameter, defined by $\alpha=R(\omega/\nu)^{1/2}$, where $\omega=2\pi/T$ is the fundamental frequency and ν is the kinematic viscosity, was 4.017 and 4.054 for the carotid bifurcation and idealized stenosis, respectively, when a high shear rate Newtonian viscosity of 3.5 cP is considered. A second-order upwind discretization scheme was applied for both the momentum and pressure equations, and the PISO scheme was used for pressure velocity coupling. A time periodic solution was achieved after three flow cycles.

It is widely recognized that the stresses exerted by the flowing blood on the walls of arteries and blood vessels are

important in maintaining good cardiovascular health and that atherosclerotic lesions appear and develop predominantly in regions where the wall shear stress is low or oscillatory (Caballero and Lain, 2015). The wall shear stress, WSS, and the modified oscillatory shear index, OSI, are commonly used in order to assess the atherogenic impact of the computed hemodynamic environment. WSS is the tangential force exerted on the arterial wall by the blood flow:

$$WSS \equiv \eta \left(\dot{\gamma} \right) \frac{\partial \mathbf{u}_t}{\partial n} \Big|_{\text{wall}} \tag{7}$$

where \mathbf{u}_t is the tangential velocity vector and n is the direction normal to the wall. OSI is used to obtain a measure of the oscillatory motion of the wall shear stress vector, as both shear vector magnitude and direction change with time in a continuous fashion. If $\boldsymbol{\tau}$ is the instantaneous wall shear stress vector and T is the heart cycle period, the mean shear direction is given by

$$\mathbf{n}_m \equiv \frac{1}{T} \int_0^T \left(\frac{\boldsymbol{\tau}}{\|\boldsymbol{\tau}\|} \right) dt \tag{8}$$

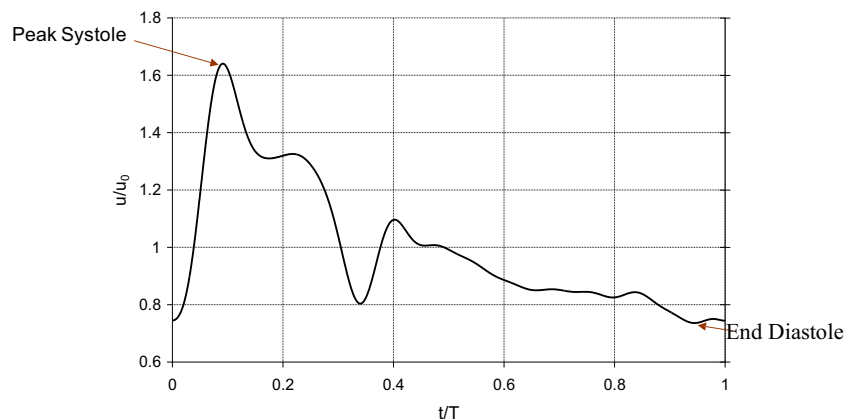
Then the modified OSI is defined by

$$OSI \equiv \frac{\int_0^T w |\boldsymbol{\tau} \cdot \mathbf{n}_m| dt}{\int_0^T |\boldsymbol{\tau} \cdot \mathbf{n}_m| dt} \tag{9}$$

where $w=0.5(1-\cos a)$ and a is the angle between $\boldsymbol{\tau}$ and \mathbf{n}_m . The values of the OSI range from 0 (unidirectional shear flow) to 0.5 (purely oscillatory shear).

From the flow curves of the two blood samples presented in Fig. 3 and the values of the dimensionless numbers presented in Table 1, it is evident that under hypoxic conditions, the measured rheological impact found is more profound in the blood sample of the female volunteer (B) compared to that of male volunteer (A). Thus, we have chosen data extracted from volunteer B to assess the influence of oxygenation level on the

Fig. 4 Flow waveform applied at the inlet of carotid bifurcation and axisymmetric stenosis models



hemodynamic environment in both the stenosis and the healthy carotid bifurcation.

Flow in an idealized axisymmetric stenosis

The shape of the idealized axisymmetric stenosis is that proposed by Tu and Deville (1996):

$$r = \begin{cases} R \left[1 - \frac{h}{2} (\cos \pi x - 1) \right], & |x| < 1 \\ R, & \text{otherwise} \end{cases} \quad (10)$$

where h is the radius at the narrowest part of the stenosis neck and R is the radius in the non-stenosed region. The post-stenotic and pre-stenotic lengths are 30 and 4 inlet diameters, respectively. Here, $h = 1.5$ mm and $R = 3$ mm to generate a 75 % by area stenosis. The computational domain was discretized with $\sim 10^4$ quadrilateral cells applying near wall refinement and modeled as an axisymmetric problem.

Figure 5 shows a comparison of axial shear stress along the stenosis wall between normal blood, oxygen-saturated and oxygen-depleted blood states for volunteer B. The largest differences appear very close to the location of maximum stenosis with oxygen-depleted blood exhibits the lowest levels of wall shear stress. Negative values of axial wall shear stress are due to the presence of post-stenotic recirculation regions. We therefore further narrow down our analysis to compare these two states in more detail. Toward this, we examine the distribution of time averaged velocity magnitude along the symmetry axis of the stenosis (Fig. 6). We note a sharper post-stenotic velocity gradient for the oxygen-saturated case as compared to the oxygen-depleted state indicating a faster post-stenotic

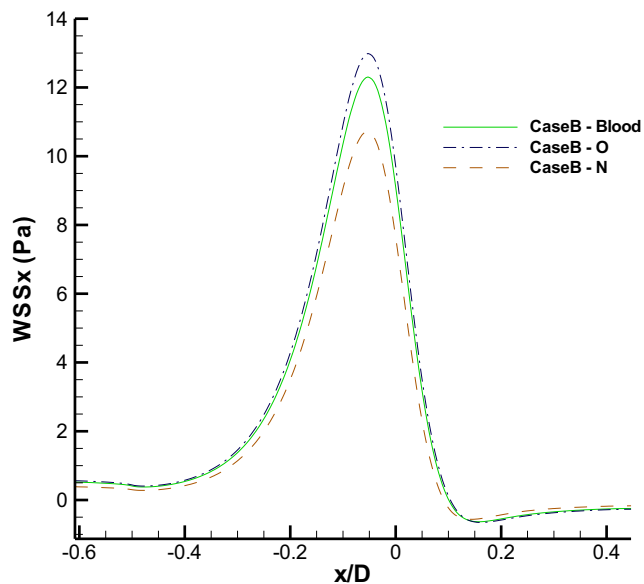


Fig. 5 Plot of time averaged axial shear stress along the stenosis wall for volunteer B. Maximum stenosis located at $x/D = 0$; *Blood*: normoxic, *O*: hyperoxic, *N*: hypoxic

recovery of the flow perturbation caused by the flow contraction and expansion caused by the stenosis. A comparison of contours of time averaged axial velocity for the oxygen-saturated and oxygen-depleted states is shown in Fig. 7. Note the significant difference in the size of the recirculation region which is clearly delineated by the zero-velocity contours. Figures 8 and 9 show snapshots of the axial velocity distribution at end-diastole and peak systole. The difference in the size of the post-stenotic recirculation regions between the two blood oxygenation states is more pronounced at the end diastolic phase with the largest regions associated with the oxygen-depleted state.

Flow in a realistic carotid bifurcation

The carotid bifurcation has been selected for our numerical hemodynamics simulations, as it is one of the most frequently studied sites evaluating the hemodynamic hypothesis of atherosclerosis (Aristokleous et al., 2011; 2015). Using a 3.0 T Philips Achieva MRI instrument, a series of thin sequential slices were obtained by 3D TOF (Time of Flight) methods, covering the right carotid artery bifurcation of a healthy volunteer in the supine position (Aristokleous et al., 2011). The inflow and outflow boundary conditions were obtained by MR phase contrast velocimetry at the limits of the TOF covered anatomic region. Segmentation and 3-D surface reconstruction of the MR images were performed using purpose-developed software. The surface of the 3-D true vessel lumen was reconstructed from the segmented TOF images. Pixel width constrained smoothing of the reconstructed surfaces was applied and smoothly matched cylindrical extensions of both inflow and outflow segments were added to facilitate the

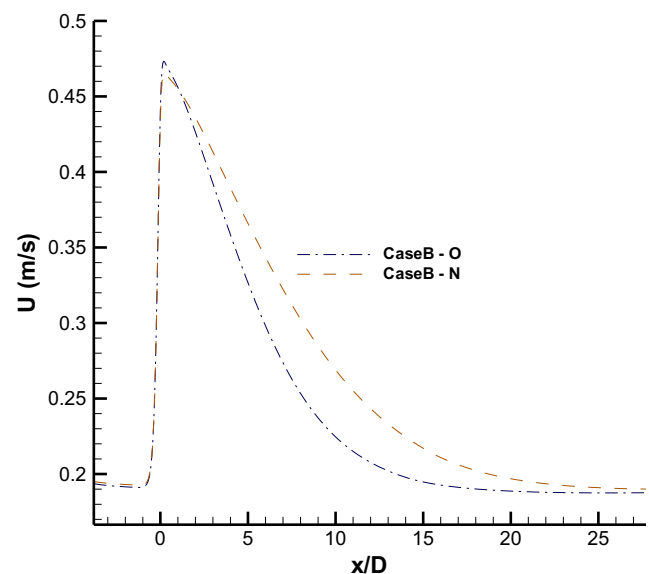


Fig. 6 Plot of averaged velocity magnitude along the symmetry axis for volunteer B. Maximum stenosis located at $x/D = 0$; *O*: hyperoxic, *N*: hypoxic

Fig. 7 Contours of time averaged axial velocity (m/s) for volunteer B. Zero-velocity contour shown in white outlines the region of flow reversal; *O*: hyperoxic, *N*: hypoxic

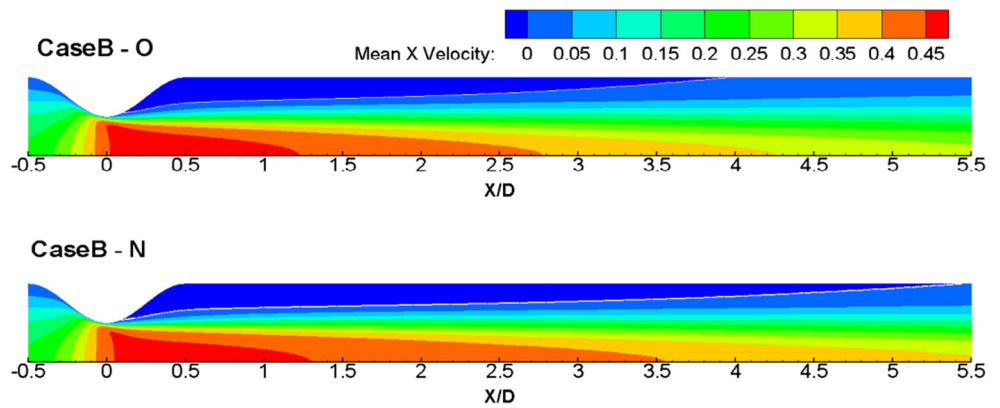
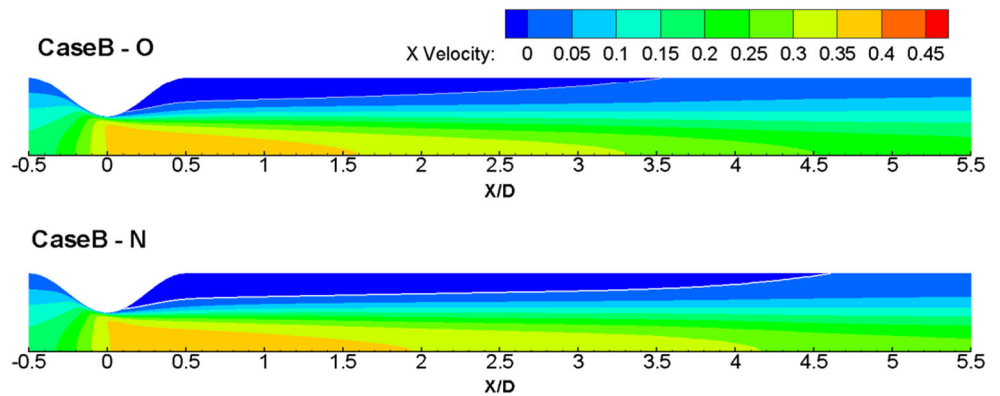


Fig. 8 Contours of axial velocity (m/s) at end-diastole for volunteer B. Zero-velocity contour shown in white outlines the region of flow reversal; *O*: hyperoxic, *N*: hypoxic



application of fully developed boundary conditions for the numerical simulation. The computational grid was generated with ANSA v12 (Beta CAE Systems, Greece) using $\sim 7.5 \cdot 10^5$ mixed type elements with higher grid density in the vicinity of the bifurcation and in the viscous layer adjacent to the wall (Aristokleous et al., 2011). A 0.65/0.35 ICA/ECA flow split was prescribed based on the in vivo MR phase contrast velocimetry measurements.

Results from the numerical computations of the flow field in the image-based physiological carotid bifurcation are presented in Figs. 10, 11, and 12 for the case of Volunteer B. The distribution of cycle averaged wall shear stress magnitude is

depicted in Fig. 10. The wall area exposed to low WSS is of importance as it provides an indication of the atherogenic impact of the flow field. It appears that the spatial extent of the low shear regions is larger in the oxygen-depleted blood state as compared to the oxygen-saturated state. Furthermore, from Fig. 11, it is evident that the wall region exposed to highly oscillating shear, as measured by the OSI, another important hemodynamic index, is also slightly higher in the oxygen-depleted state. Finally, regions of recirculation in the context of the cycle averaged velocity field are depicted in Fig. 12 as zero axial velocity iso-surfaces. Differences in the spatial extent of the recirculation regions between the oxygen-

Fig. 9 Contours of axial velocity (m/s) at peak systole for Volunteer B. Zero-velocity contour shown in white outlines the region of flow reversal; *O*: hyperoxic, *N*: hypoxic

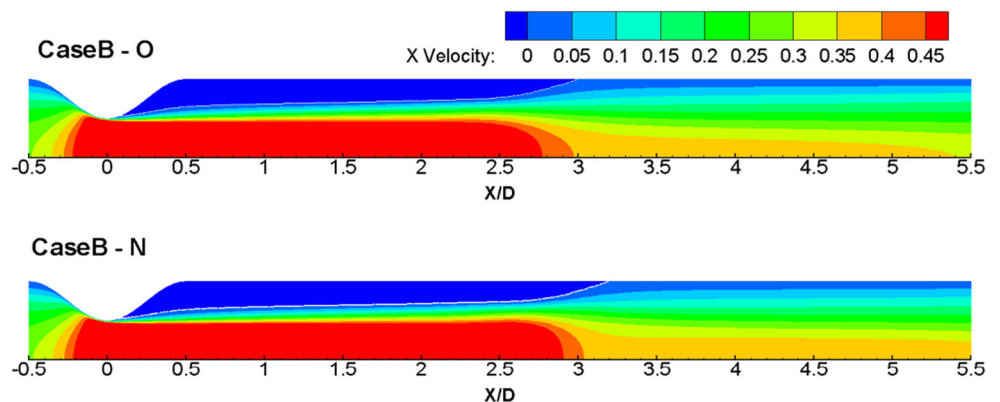
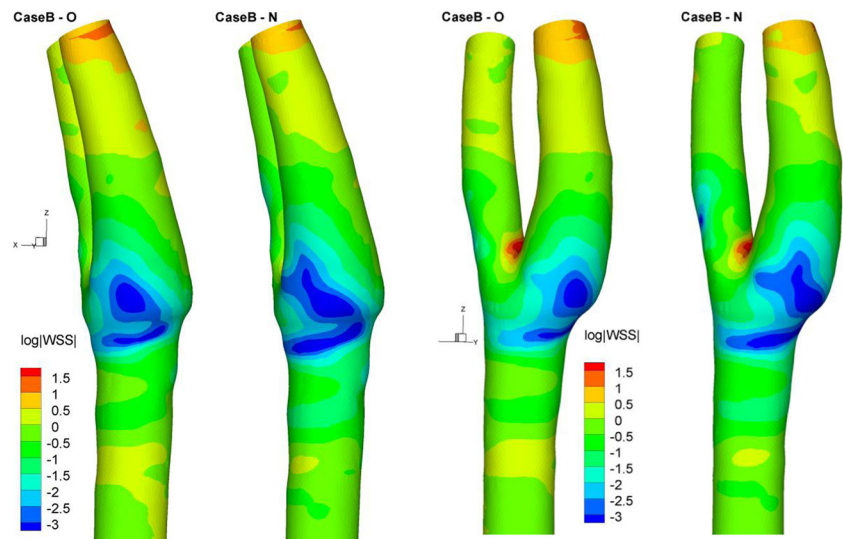


Fig. 10 Contours of log time averaged wall shear stress magnitude in blood flow in a carotid bifurcation (volunteer B); *O*: hyperoxic, *N*: hypoxic



saturated and oxygen-depleted states are not readily appreciated.

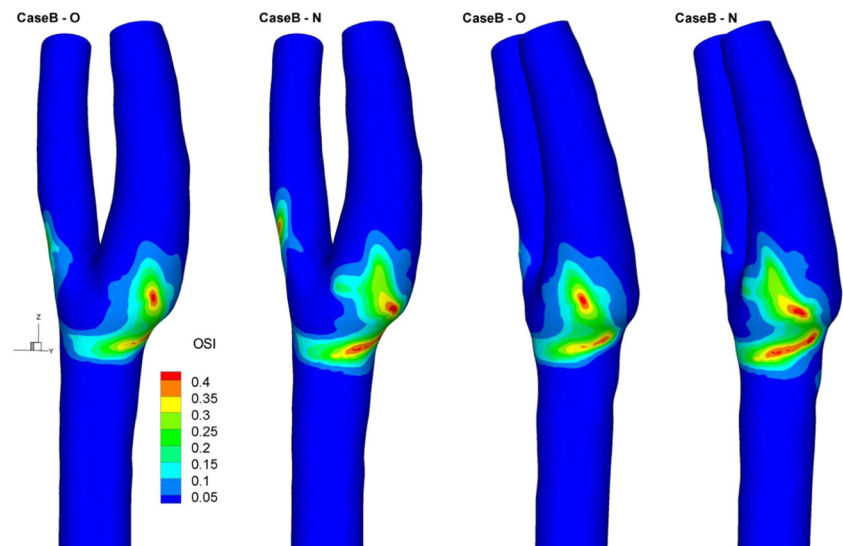
Concluding remarks

In order to study the effect of oxygen concentration on blood rheology, rheological measurements on two blood samples (from a male and a female) have been carried out at different oxygenation levels: oxygen-depleted, regular, and oxygen-saturated blood. The rheological data were fitted to the Herschel-Bulkley constitutive equation. Oxygen-induced changes of the rheological parameters were less pronounced in the case of the higher hematocrit (male) blood sample. Hence, numerical simulations of blood flow were carried out only for the lower hematocrit (female) sample. Results have

been obtained for flow in an idealized stenosis geometry and in a realistic carotid bifurcation.

Blood without oxygen (hypoxic) was found to have lower viscosity while blood saturated with oxygen (hyperoxic) has higher viscosity than normal (normoxic) human blood. This finding is obviously relevant to acute rather than chronic hypoxia although both conditions have been reported to increase blood viscosity in animal experiments, i.e., Yelmen et al. (2011), Núñez-Espinosa et al. (2014), and Kang et al. (2016), Kohl et al. (2015) with the exception of Esteva et al. (2009) who found that the apparent blood viscosity is not affected. The viscosity increase in these cases could be explained by the deformability of red blood cells, which depends on the oxygen content in hemoglobin. The difference observed between our results, based on experiments conducted in vitro, and those reported in the literature conducted in vivo may indicate that the effect of hypoxia on the rheological

Fig. 11 Contours of Oscillatory Shear Index (OSI) in blood flow in a carotid bifurcation (volunteer B); *O*: hyperoxic, *N*: hypoxic



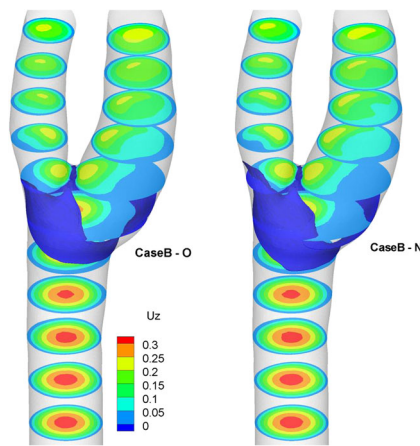


Fig. 12 Contours of time averaged axial velocity on cross sections normal to the z -axis and zero-velocity iso-surfaces in blood flow in a carotid bifurcation (volunteer B); *O*: hyperoxic, *N*: hypoxic

properties of blood results from a complex physiological response that was not replicated *in vitro*. Therefore, the presented numerical simulations should be simply viewed as a supplement to the experimental *in vitro* measurements. More work is required in order to simulate the effects of oxygen on blood flow in a realistic carotid bifurcation. For example, the effects on blood viscoelasticity and thixotropy and also on the arterial wall properties should be taken into account. In any case, the purpose of the simulations in a realistic carotid bifurcation arterial segment model was to elucidate differences in rheology due to geometry and near wall parameters such as the wall shear stress distribution and to see if changes in oxygen concentration and as a result changes in blood viscosity have a significant effect on the velocity distribution and the wall shear stress.

Oxygen availability is a critical factor to metabolically regulate systemic and peripheral blood flow (*in vivo* regulation). Interestingly, in the *in vivo* experiments on mice microcirculation, hypoxic blood (10 % oxygen) decreased the blood flow through the peripheral blood vessels, while hyperoxia (100 % oxygen) increased it in comparison to normoxia (20 % oxygen) (Jia, 2011). To elaborate further on our findings, there is a rationale—on the blood capillary level—to observe that hypoxic blood exhibited lower viscosity (our *in vitro* finding) since there is a decreased blood flow (of hypoxic blood) through peripheral blood vessels (*in vivo* finding on C57BL/6 adults mice), and vice versa is true for hyperoxic blood. However, in some blood vessels, such as coronary arteries or cerebral blood vessels, hyperoxia can be considered as a strong vasoconstrictor stimulus (Farquhar, 2009).

On the level of carotid bifurcation, rheological properties are important to evaluate the oxygen transport between the blood and artery wall tissue (oxygen diffusion in the artery wall). Differences in the blood flow pattern can lead to changes in oxygen tension and oxygen wall flux (Tada, 2010). It is important to notice that in urgent clinical situations, such as

stroke, traumatic brain injury, or acute coronary syndromes, high-concentration oxygen therapy is considered an important interventional procedure. Due to the vasoconstriction property of hyperoxic blood on cerebral blood vessels and coronary arteries, and combined with the observation that hyperoxic blood exhibits higher viscosity (our findings), it is clear that we need further studies to address the safety of this conventional clinical approach. Also, blood hypoxia is quite commonly observed in physiological conditions (local perfusion of skeletal muscles during physical activity) or under pathological conditions (ischemia after stroke or acute myocardial infarction).

Although oxygen concentration affects the rheological properties of blood, these changes do not, however, appear to have a strong impact on the hemodynamic environment in the carotid bifurcation. Among the cases considered, the most notable effect was found when the blood sample of volunteer B was oxygen depleted by nitrogen saturation (Case B-N). Figures 10 and 11 show an increase in the wall area exposed to low WSS and high OSI, respectively, resulting from oxygen depletion in the blood sample. An increase in the flow reversal region is noted in Fig. 12.

The results in the idealized axisymmetric stenosis model indicate that there is an effect on the velocity field due to changes in the rheological properties of blood which is most notable between Case B-O and Case B-N. The reduction in the WSS in Case B-N as compared to the oxygen-saturated state (Case B-O) can be explained by the associated significant reduction in the characteristic viscosity shown in Table 2. It is also interesting to note the increase in the size of the post-stenotic recirculation region due to the oxygen depletion shown in Figs. 8 and 9.

Acknowledgments We are grateful to the two referees for their constructive comments and criticism. This work was partially funded by a bilateral Cyprus–Slovenia grant from the Cyprus Research Promotion Foundation and the Slovenia Research Agency under the program “DESMI 2009–2010” (Title: The fluidity of blood at different levels of oxygen content; Project: DIAKRATIKES/KY-SLO/0411/02) of the framework program “for research, technological development and innovation 2009–2010” co-funded by the Republic of Cyprus and the European Regional Development Fund.

References

- Apostolides AJ, Beris AN (2014) Modeling of the blood rheology in steady-state shear flows. *J Rheol* 58:607–633
- Apostolides AJ, Armstrong MJ, Beris AN (2015) Modeling of human blood rheology in transient shear flows. *J Rheol* 59:275–298
- Apostolides AJ, Beris AN (2016) The effect of cholesterol and triglycerides on the steady state shear rheology of blood. *Rheol Acta* 55:497–509
- Aristokleous N, Seimenis I, Papaharilaou Y, Georgiou G, Brott BC, Anayiotos AS (2011) Effect of posture change on the geometric

- features of the healthy carotid bifurcation. *IEEE Trans Inf Tech Biomed* 15:148–154
- Aristokleous N, Seimenis I, Georgiou GC, Nicolaides A, Anayiotos AS (2015) The effect of head rotation on the geometry and hemodynamics of healthy vertebral arteries. *Ann Biomed Eng* 43:1287–1297
- Balmforth NJ, Frigaard IA, Ovarlez G (2014) Yielding to stress: recent developments in viscoplastic fluid mechanics. *Annu Rev Fluid Mech* 46:121–46
- Barnes HA (1999) The yield stress—a review or ‘παντα ρει’—everything flows? *J Non-Newtonian Fluid Mech* 81:133–178
- Benderro GF, LaManna JC (2013) Kidney EPO expression during chronic hypoxia in aged mice. *Adv Exp Med Biol* 765:9–14
- Bertoluzzo SM, Bollini A, Rasia M, Raynal A (1999) Kinetic model for erythrocyte aggregation. *Blood Cells Mol Dis* 25:339–349
- Bessonov N, Sequeira A, Simakov S, Vassilevskii Y, Volpert V (2016) Methods of blood flow modelling. *Math Model Nat Phenom* 11:1–25
- Brun JF, Varlet-Marie E, Romain AJ, Guiraudou M, Raynaud de Mauverger E (2013) Exercise hemorheology: moving from old simplistic paradigms to a more complex picture. *Clin Hemorheol Microcirc* 55:15–27
- Brust M, Schaefer C, Doerr R, Pan L, Garcia M, Arratia PE, Wagner C (2013) Rheology of human blood plasma: Viscoelastic versus Newtonian behavior. *Phys Rev Lett* 110:078305
- Butler IB, Schoonen MA, Rickard DT (1994) Removal of dissolved oxygen from water: a comparison of four common techniques. *Talanta* 41:211–215
- Caballero AD, Lain S (2015) Numerical simulation of non-Newtonian blood flow dynamics in human thoracic aorta. *Comp Meth Biomech Biomed Eng* 18:1200–1216
- Caillaud C, Connes P, Bouix D, Mercier J (2002) Does haemorheology explain the paradox of hypoxemia during exercise in elite athletes or thoroughbred horses? *Clin Hemorheol Microcirc* 26:175–181
- Chien S, Usami S, Dellenback RJ, Gregersen MI (1967) Blood viscosity: influence of erythrocyte aggregation. *Science* 157:827–829
- Cokelet G, Merrill EW, Gilliland ER, Shin H, Britten A, Wells RE (1963) The rheology of human blood—measurement near and at zero shear rate. *Trans Soc Rheol* 7:303–317
- Copley AI, Huang CR, King RG (1973) Rheogoniometric studies of whole human blood at shear rates from 1000 to 0.0009 sec⁻¹. I. Experimental findings. *Biogeosciences* 10:17–22
- De Cort SC, Innes JA, Barstow TJ, Guz A (1991) Cardiac output, oxygen consumption, and arteriovenous oxygen difference following a sudden rise in exercise level in humans. *J Physiol* 441:501–512
- Diaw M, Samb A, Diop S, Sall ND, Ba A, Cissé F, Connes P (2014) Effects of hydration and water deprivation on blood viscosity during a soccer game in sickle cell trait carriers. *Br J Sports Med* 48:326–331
- Dimakopoulos Y, Kelesidis G, Tsouka S, Georgiou GC, Tsamopoulos J (2015) Hemodynamics in stenotic microvessels under steady state conditions. Part I: the non-homogeneous model. *J Biorheol* 52:183–210
- Dintenfass L (1962) Thixotropy of blood and proneness to thrombus formation. *Circ Res* 11:233–239
- Dintenfass L (1971) *Blood Microrheology—Viscosity Factors in Blood Flow, Ischaemia and Thrombosis*, Butterworth
- Esteva S, Panisello P, Torrella JR, Pages T, Viscor G (2009) Blood rheology adjustments in rats after a program of intermittent exposure to hypobaric hypoxia. *High Alt Med Biol* 10:275–281
- Farquhar H, Weatherall M, Wijesinghe M, Perrin K, Ranchord A, Simmonds M, Beasley R (2009) Systematic review of studies of the effect of hyperoxia on coronary blood flow. *Am Heart J* 158:371–377
- Fedosov DA, Pan W, Caswell B, Gompper G, Karniadakis GE (2011) Predicting human blood viscosity in silico. *PNAS* 108:11772–11777
- Guner I, Uzun DD, Yaman MO, Genc H, Geligsen R, Korkmaz GG, Hallac M, Yelmen N, Sahin G, Karter Y, Simsek G (2013) The effect of chronic long-term intermittent hypobaric hypoxia on bone mineral density in rats: role of nitric oxide. *Biol Trace Elem Res* 154:262–267
- Jia Y, Li P, Dziennis S, Wang RK (2011) Responses of peripheral blood flow to acute hypoxia and hyperoxia as measured by optical microangiography. *PLoS One* 6:e26802
- Kang J, Li Y, Hu K, Lu W, Zhou X, Yu S, Xu L (2016) Chronic intermittent hypoxia versus continuous hypoxia: same effects on hemorheology? *Clin Hemorheol Microcirc*. doi:10.3233/CH-151973
- Kim S, Namgung B, Ong PK, Cho YI, Chun KJ, Lim D (2009) Determination of rheological properties of whole blood with a scanning capillary-tube rheometer using constitutive models. *J Mech Sci Technol* 23:1718–1726
- King MW (2015) Hemoglobin and Myoglobin. <http://themedicalbiochemistrypage.org/hemoglobin-myoglobin.php#myoglobin>
- Kohl ZF, Crossley DA II, Tazawa H, Burggren WW (2015) Dynamics of blood viscosity regulation during hypoxic challenges in the chicken embryo (*Gallus gallus domesticus*). *Comp Biochem Physiol A Mol Integr Physiol* 190:1–8
- Longo V, D’Alessandro A, Zolla L (2014) Deoxygenation of leucofiltered erythrocyte concentrates preserves proteome stability during storage in the blood bank. *Blood Transfus* 12:599–604
- Lykov K, Li X, Lei H, Pivkin IV, Karniadakis GE (2015) Inflow/outflow boundary conditions for particle-based blood flow simulations: application to arterial bifurcations and trees. *PLoS Comput Biol* 11:e1004410
- Merrill EW, Cheng CS, Pelletier GA (1969) Yield stress of normal human blood as a function of endogenous fibrinogen. *J Appl Physiol* 26:1–3
- Mitsoulis E (2007) Flows of viscoplastic materials: models and computation. *Rheol Reviews* 2007:135–178
- Núñez-Espinosa C, Douziech A, Ríos-Kristjánsson JG, Rizo D, Torrella JR, Pagé T, Viscor G (2014) Effect of intermittent hypoxia and exercise on blood rheology and oxygen transport in trained rats. *Respir Physiol Neurobiol* 192:112–117
- Papanastasiou TC (1987) Flow of materials with yield. *J Rheol* 31:385–404
- Picart C, Piau JM, Galliard H, Carpentier P (1998) Blood low shear rate rheometry: influence of fibrinogen level and hematocrit on slip and migrational effects. *Biorheology* 35:335–353
- Picart C, Carpentier PH, Galliard H, Piau JM (1999) Blood yield stress in systemic sclerosis. *Am J Physiol Heart Circ Physiol* 276:771–777
- Popel AS, Johnson PC (2005) Microcirculation and hemorheology. *Annu Rev Fluid Mech* 37:43–69
- Rand PW, Lacombe E, Hunt HE, Auston WH (1964) Viscosity of normal; human blood under normothermic and hypothermic conditions. *J Appl Physiol* 19:117–122
- Smith MM, Lucas AR, Hamlin RL, Devor ST (2015) Associations among hemorheological factors and maximal oxygen consumption. Is there a role for blood viscosity in explaining athletic performance? *Clin Hemorheol Microcirc* 60:347–362
- Sousa PC, Pinho FT, Alves MA, Oliveira MSN (2016) A review of hemorheology: measuring techniques and recent advances. *Korea-Australia Rheol J* 28:1–22
- Tada S (2010) Numerical study of oxygen transport in a carotid bifurcation. *Phys Med Biol* 55:3993–4010
- Thurston GB (1996) Viscoelastic properties of blood and blood analogs. *Adv Hemodynamics Hemorheol* 1:1–30
- Tu C, Deville M (1996) Pulsatile flow of non-Newtonian fluids through arterial stenoses. *J Biomech* 29:899–908

- Valant AZ, Zibera L, Papaharilaou Y, Anayiotos A, Georgiou GC (2011) The influence of temperature on rheological properties of blood mixtures with different volume expanders—implications in numerical arterial hemodynamics simulations. *Rheol Acta* 50:389–402
- Vlastos G, Lerche D, Koch B, Samba O, Pohl M (1997) The effect of parallel combined steady and oscillatory shear flows on blood and polymer solutions. *Rheol Acta* 36:160–172
- Yelmen N, Ozdemir S, Guner I, Toplan S, Sahin G, Yaman OM, Sipahi S (2011) The effects of chronic long-term intermittent hypobaric hypoxia on blood rheology parameters. *Gen Physiol Biophys* 30:389–395
- Yeow YL, Wickramasinghe SR, Leong YK, Han B (2002) Model independent relationships between hematocrit, blood viscosity, and yield stress derived from Couette viscometry data. *Biotechnol Prog* 18:1068–1075
- Zhang M, Li XM, Feng J, Xu GJ, Liu XB, Jiang H, Niu CY, Zhao ZG (2012) Changes of blood viscosity and erythrocyte rheology in acute hypoxic hypoxia mice. *Chin J Appl Physiol* 28:454–457
- Zolla L, D'Alessandro A (2013) An efficient apparatus for rapid deoxygenation of erythrocyte concentrates for alternative banking strategies. *J Blood Transfusion* 2013:896537